

Author's Accepted Manuscript

Novel adaptation of the demodulation technology for gear damage detection to variable amplitudes of mesh harmonics

F. Combet, L. Gelman

PII: S0888-3270(10)00244-X
DOI: doi:10.1016/j.ymsp.2010.07.008
Reference: YMSSP 2619

To appear in: *Mechanical Systems and Signal*

Received date: 29 August 2008
Revised date: 8 June 2010
Accepted date: 18 July 2010

Cite this article as: F. Combet and L. Gelman, Novel adaptation of the demodulation technology for gear damage detection to variable amplitudes of mesh harmonics, *Mechanical Systems and Signal*, doi:10.1016/j.ymsp.2010.07.008

This is a PDF file of an unedited manuscript that has been accepted for publication. As a service to our customers we are providing this early version of the manuscript. The manuscript will undergo copyediting, typesetting, and review of the resulting galley proof before it is published in its final citable form. Please note that during the production process errors may be discovered which could affect the content, and all legal disclaimers that apply to the journal pertain.



www.elsevier.com/locate/ymsp

Novel adaptation of the demodulation technology for gear damage detection to variable amplitudes of mesh harmonics

F. Combet, L. Gelman

Cranfield University, Cranfield, MK43 0AL, UK

Tel. 01234 750111ext.5425, fax 01234 754797email: l.gelman@cranfield.ac.uk

Abstract

In this paper, a novel adaptive demodulation technique including a new diagnostic feature is proposed for gear diagnosis in conditions of variable amplitudes of the mesh harmonics. This vibration technique employs the time synchronous average (TSA) of vibration signals. The new adaptive diagnostic feature is defined as the ratio of the sum of the sideband components of the envelope spectrum of a mesh harmonic to the measured power of the mesh harmonic. The proposed adaptation of the technique is justified theoretically and experimentally by the high level of the positive covariance between amplitudes of the mesh harmonics and the sidebands in conditions of variable amplitudes of the mesh harmonics. It is shown that the adaptive demodulation technique preserves effectiveness of local fault detection of gears operating in conditions of variable mesh amplitudes.

1. Introduction

Local tooth damage produces short-duration impacts that add modulation effects to the meshing vibration, and in turn generate a higher level of sidebands (SB) around the mesh harmonics [1]. The vibration demodulation analysis has been widely investigated [1-14] detecting local tooth damage such as cracks, pitting, etc. However, previous works have not considered how the technique works with the time synchronous average (TSA) [15] of vibration signals under conditions of variable amplitudes of the mesh harmonics and their surrounding sidebands [1]. The variation of mesh amplitudes deteriorates the diagnostic effectiveness of the method [8].

An original method and a new diagnostic feature were proposed [8] for conditions of variable mesh amplitudes. The method is based on the high level of positive covariance between amplitudes of the mesh harmonics and their surrounding SB: amplitudes of the SB vary in proportion to amplitudes of the mesh harmonics. This positive covariance for non-TSA raw vibrations was found [8] theoretically and experimentally for the first time.

The diagnostic feature proposed in ref. [8] is based on the normalized sum of SB and estimated on the non-TSA *raw* vibrations. However, in order to increase the signal/noise ratio and perform effectively differential gear diagnosis, it is generally preferred to perform demodulation on the TSA signals.

Therefore, the problem is to improve the classical demodulation technique based on the TSA gear vibrations in conditions of variable mesh amplitudes. This problem is not investigated in the existing literature nor has the covariance between amplitudes of the sidebands and the mesh harmonics for the TSA gear vibrations been investigated.

Thus, the aims of this short communication are to

- investigate theoretically and experimentally the covariance between amplitudes of the mesh harmonics and the sidebands estimated from the TSA gear signals
- improve the demodulation technique in conditions of variable amplitudes of the mesh harmonics
- compare experimentally the novel adaptive demodulation technique with the classical demodulation technique for local damage detection in gearboxes

In section 2, the theoretical covariance between amplitudes of the mesh and the sum of the SB components is investigated based on a model of the TSA signal. In section 3, the experimental set-up is described, and the covariance between amplitudes of the mesh and the sum of the SB components is investigated based on experimental measurements. In section 4, a novel adaptive demodulation technique is proposed and investigated. Conclusions are drawn in section 5.

2. Theoretical analysis of the covariance between the mesh and the sidebands

The TSA signal of a gear may be modeled as [3, 4]:

$$x(t) = \sum_{k=1}^K X_k (1 + a_k(t)) \cos(2\pi k f_m t + \varphi_k(t)), \quad (1)$$

where $a_k(t)$ and $\varphi_k(t)$ are the amplitude and phase modulation functions and X_k is the amplitude of the mesh harmonic k .

After band-pass filtering around the mesh harmonic k with appropriate bandwidth for including all modulation sidebands but excluding interferences from adjacent mesh harmonics [3], by using the Hilbert transform, we obtain the complex signal:

$$z_k(t) = X_k(1 + a_k(t))\exp(j2\pi k f_m t + \varphi_k(t)) \quad (2)$$

The envelope (amplitude modulation) is obtained from its modulus:

$$|z_k(t)| = X_k(1 + a_k(t)) \quad (3)$$

The envelope spectrum is then computed as:

$$PSD_e = |X_k(\delta(f) + A_k(f))|^2, \quad (4)$$

where $\delta(f)$ is the Dirac function and $A_k(f)$ is the Fourier transform of amplitude modulation function $a_k(t)$.

The sum of the sideband components for the mesh harmonic k is estimated from the envelope spectrum as:

$$SUMSB_k = X_k^2 \sum_{f=1}^{SBnbr} |A_k(f)|^2, \quad (5)$$

where $SBnbr$ is the number of the sidebands, corresponding to half the bandwidth of the bandpass filter applied to the mesh harmonic.

The sideband power can be also extracted from the spectrum of synchronously averaged gear signals.

If the number of the sidebands $SBnbr$ is high enough to encompass all sideband components of the amplitude modulation function $a_k(t)$, this may also be expressed by using Parseval's theorem as:

$$SUMSB_k = X_k^2 \frac{1}{T} \sum_{t=0}^T |a_k(t)|^2 = X_k^2 P_{ak}, \quad (6)$$

where T is the shaft period and P_{ak} is the mean power of the amplitude modulation function. When the operating conditions (load and speed) are varying, the amplitude X_k of the mesh harmonic k and its surrounding sidebands are affected [1]. Therefore, the sum of the sidebands in equation (6) should vary in direct proportion to the mesh power, i.e., the covariance between the two should be positive. The cross-covariance coefficient (i.e. the normalized covariance) is estimated as

$$\text{cov}[X_k^2; \text{SUMSB}_k] = \frac{C[X_k^2; \text{SUMSB}_k]}{\sqrt{C[X_k^2; X_k^2] \cdot C[\text{SUMSB}_k; \text{SUMSB}_k]}}, \quad (7)$$

where $C[X; Y]$ represents the un-normalised cross-covariance between the two random variables X and Y .

Ideally, this normalized covariance between the mesh harmonic and sum of the SB should be close to unity [8]. If this is not the case, this deviation could be due to interfering components which are included in the demodulation bandwidth but are not related to the modulation process, or to the effect of the transmission path on gear vibration [16].

3. Experimental analysis of the covariance between the mesh and the sidebands

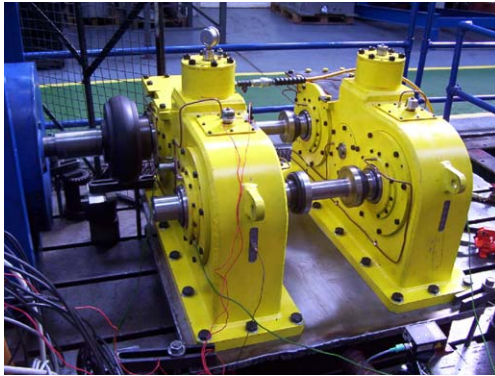
3.1 Experimental set-up

The gear system under experiment is a back-to-back system designed by Compact Orbital Gears (UK). The back-to-back arrangement is composed of two identical spur gearboxes, each one containing two gears with 60 teeth and in between a 59 tooth idle pinion. Figure 1 shows the system under experiment and a schematic of one of the gearboxes. The loading of the system is created by a piston at the top of the gearbox, which is mechanically bonded to the rotation axis of the pinion. When the piston chamber is pressurized, the pinion is pushed upwards (or downwards) with a specific force F , inducing in turn a vertical force $F/2$ on the teeth of the two gears on both sides of the pinion. The effect is to create a torque which transmits from one gear to the other through the pinion and circulates from one gearbox to the other. The torque losses in the system are compensated by the driving motor.

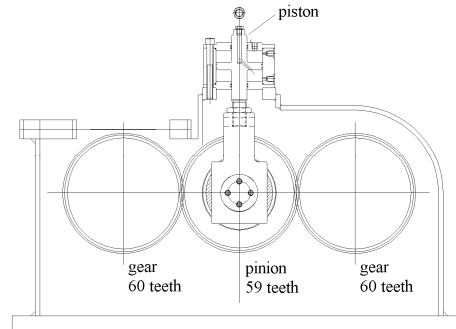
The experiment was conducted in two steps. Vibration measurements were first captured for brand new gears and then with a pitting fault which was created on one tooth of one of the gear wheels with 60 teeth. The pitting fault is a localized pitting with a 10% relative pitting

size. The relative pitting size was estimated as the pitted area divided by the tooth face area; tooth dimensions are 12mm in height and 110mm in width. Only the acceleration measurements in the vertical direction were processed here.

From the pressure reading above the piston, the torque in the system was roughly estimated. The experiment was conducted at different levels of load; the full load conditions (10bar pressure) correspond to about 750Nm torque.



a) The back-to-back system of two identical coupled gearboxes



b) Schematic of one of the gearboxes

Fig. 1 Experimental setup

3. 2. Experimental results

Experiments were performed for different operating conditions of the gearbox: near full load, 500rpm, 700rpm and 1400rpm speed and near half load, 700rpm, 1050rpm and 1300rpm speed, in the un-pitted and pitted conditions of the gear. For each case, the measured signal was split into several realizations of 50s duration, and the TSA was performed on this duration of gear vibrations.

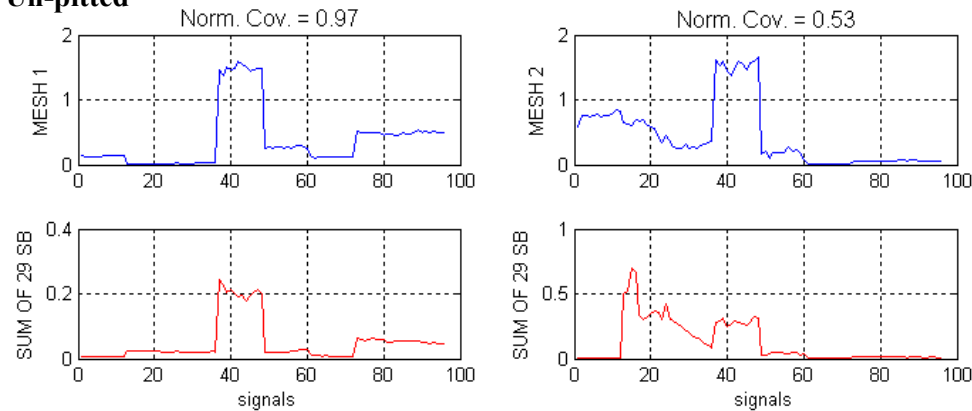
For the first two mesh harmonics, their respective sums of SB (SUMSB) is estimated from the envelope spectrum as described in section 2 (i.e., Eq.(5)). The powers of the mesh harmonics are estimated from the spectrum of the TSA signal. The number of the SB is varied from 1 to a maximum of 29 SB corresponding to almost half the mesh frequency [2].

The covariance between the mesh power and the sum of the SB is investigated when combining together all signals corresponding to all operating conditions. Figure 2 shows the variations of the power of the mesh harmonics 1 and 2 and of the sum of 29 SB in the un-pitted (top) and pitted (bottom) cases. A high positive normalised covariance (close to unity) is observed for the mesh harmonic 1 in both the un-pitted and pitted conditions. For the mesh

harmonic 2, however, the covariance is lower, mainly due to the opposite variations of the mesh and the SB occurring around signals 0-12 for the un-pitted conditions and signals 0-37 for the pitted conditions

This effect may be attributed to some interfering effects due to the transmission path (i.e., local resonances, etc.) affecting this mesh and its sidebands [16].

Un-pitted



Pitted

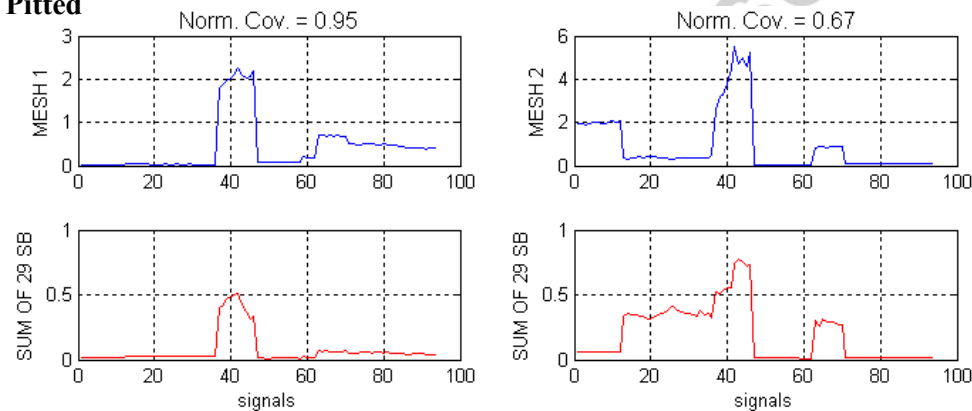


Fig. 2. The covariance between the power of the mesh harmonic and the sum of 29 sidebands for the first (left) and the second (right) mesh harmonics for a combination of signals measured under different load and speed conditions; top plots are for the un-pitted conditions, bottom plots are for the pitted conditions. The normalised covariance is indicated in the title.

Figure 3 shows dependencies of the normalized covariance between the power of the mesh harmonics and the sum of the sidebands for different number of the SB from 1 to 29. The covariance appears to be little dependent on the number of the SB here.

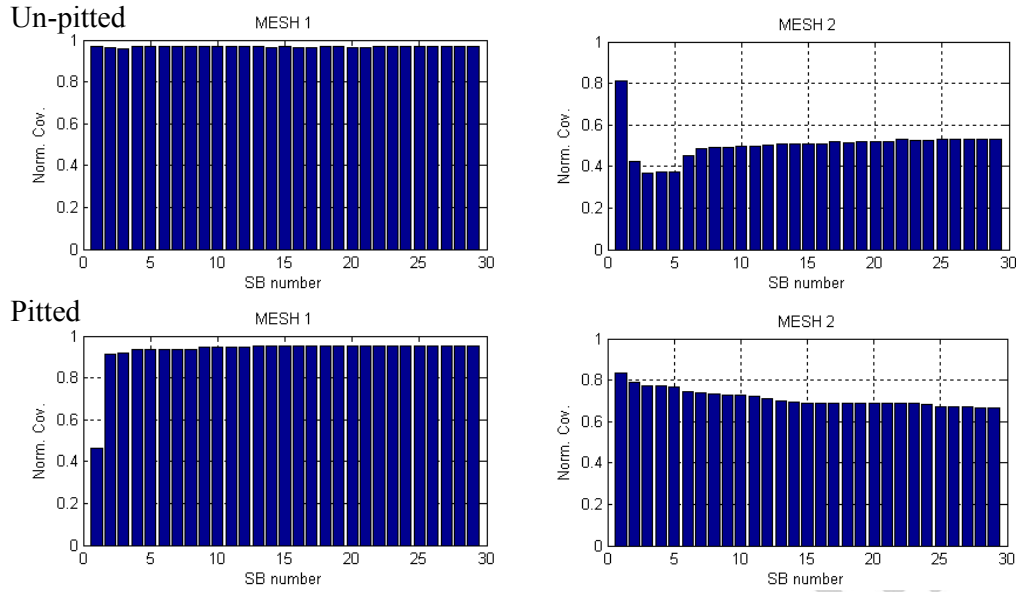


Fig. 3. Dependencies of the normalised covariance between the power of the mesh harmonic and the sum of the sidebands for the first (left) and the second (right) mesh harmonics and for different number of the sidebands, from 1 to 29; top plots are for the un-pitted conditions, bottom plots are for the pitted conditions.

4. Adaptive demodulation technique

It is known that amplitudes of the mesh harmonics and their surrounding sidebands are affected by the changes in operating conditions (i.e., load and speed) of a gear [1]. Therefore, a diagnostic feature based on the absolute amplitudes of the sidebands such as the $SUMSB_k$ (Eq.(5)) is not reliable [8] under varying operating conditions, i.e. of variable mesh amplitudes.

Based on the high level of the covariance between the mesh power and the sum of the SB amplitudes proved theoretically in section 2 and observed experimentally in section 3, one can conclude that the powers of mesh harmonics are nuisance parameters [17-18] for the classical demodulation technology. It is known [17-18] that changes of nuisance parameters lead to deterioration of the detection effectiveness.

To preserve the detection effectiveness of the classical demodulation technique in conditions of variable mesh harmonics, an adaptation of the demodulation technique to variable mesh amplitudes is proposed here. The proposed generic adaptive demodulation technique is based on synchronous measurement of the non-adaptive diagnostic feature, the sum of the SB amplitudes, and the measurable nuisance parameter, the power of the mesh harmonic, and

continuous adaptation of the technique to changes of the power of the mesh harmonic. The proposed adaptation is performed by estimating a new adaptive diagnostic feature called the $SBratio_k$ and defined by

$$SBratio_k = \frac{SUMSB_{km}}{X_{km}^2}, \quad (8)$$

where the $SUMSB_{km}$ is the measured sum of the SB related to kth mesh harmonic, X_{km}^2 is the measured power of the kth mesh harmonic.

It should be highlighted that the proposed adaptation is expedient only if amplitudes of the mesh harmonics are variable.

The adaptive demodulation technique is compared with the classical demodulation technique for experimental detection of gear pitting. The benefit of the adaptive demodulation technique is evaluated by a detection effectiveness criterion. The Fisher criterion (FC) [19] is used here; this criterion could measure separation between diagnostic features for the un-pitted and pitted conditions.

Figure 4 shows the non-adaptive (i.e. equation (5)) and the adaptive (i.e. equation (8)) diagnostic features for the mesh harmonics 1 and 2 obtained experimentally for 500rpm gear speed.

It can be seen from Figure 4 that both techniques could perform effective early differential detection of local tooth fault. The adaptation dramatically improves fault detection for the mesh harmonic 1: the FC increases from 175 to 1098 (i.e., 6.3 times increment); however, for the mesh harmonic 2, the FC slightly decreases from 386 to 268 (i.e., 1.4 times decrement).

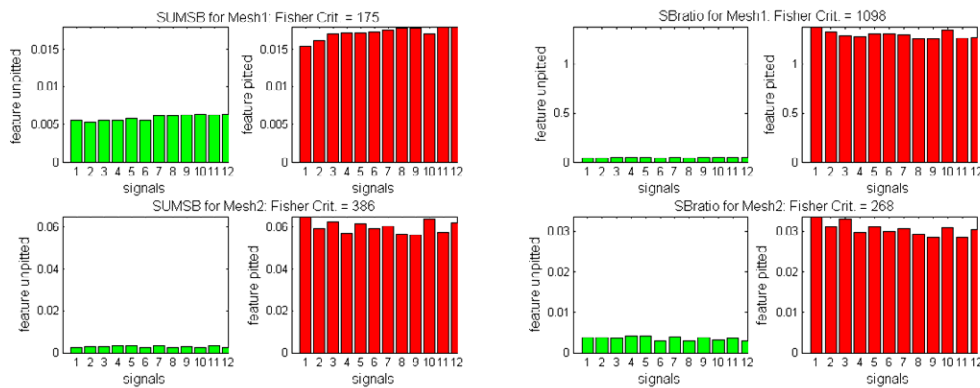


Fig. 4. The non-adaptive (left) and the adaptive (right) diagnostic features estimated for the mesh harmonics 1 and 2 in the un-pitted and pitted conditions for the full load and 500rpm speed.

To explain these detection results, Figure 5 shows the distribution of the measured power of the mesh harmonics in the un-pitted and pitted conditions of the gear. It appears that the power of the mesh harmonic 1 has decreased between the experiments in the un-pitted and pitted conditions. This is due to 20% decrease in load for pitted conditions. The power of the mesh harmonic 2 depends on the power of the mesh harmonic 1 and the gearbox level of non-linearity and has increased between the experiments in the un-pitted and pitted conditions due to increase of gearbox level of non-linearity. This Figure illustrates the high sensitivity of the powers of the mesh harmonics to changes of operating conditions,

The difference in the powers of the mesh harmonic 1 deteriorates the detection effectiveness of the non-adaptive diagnostic feature. This is because the mesh powers for the un-pitted case are greater than the mesh powers in the pitted case.

The difference in the powers of the mesh harmonic 2 improves the detection effectiveness of the non-adaptive diagnostic feature. This is because the mesh powers for the un-pitted case are less than the mesh powers in the pitted case.

However, this improvement is misleading and based purely on the difference in the powers of the mesh harmonic 2 and high positive covariance between the mesh power and the SB amplitudes.

In order to preserve the detection effectiveness in both considered cases, one needs to use the proposed adaptive demodulation technique which essentially eliminates influence of the variable mesh powers.

Thus, the experimental results have clearly shown the necessity of technique adaptation by using the adaptive diagnostic feature. This adaptation eliminates the influence of variable mesh powers on the detection effectiveness and therefore, preserves effectiveness of local fault detection of gears operating in conditions of variable mesh amplitudes.

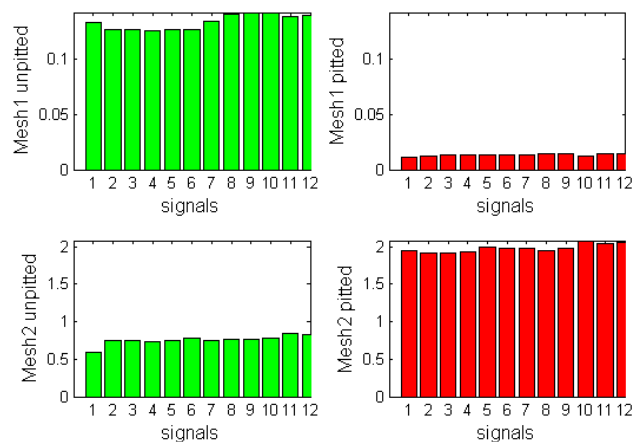


Fig. 5. Mesh power distributions for the un-pitted (left) and pitted (right) conditions of the gear for the first and the second mesh harmonics.

5. Conclusions

1. A high level of the positive covariance between amplitudes of the mesh harmonics and sidebands is found for the first time, theoretically and experimentally, for the time synchronous averaged (TSA) gear vibrations.
2. A novel generic adaptive demodulation of the TSA gear signals is proposed and investigated for local damage detection in gears in conditions of variable mesh amplitudes. The proposed vibration technique is based on synchronous measurement of the non-adaptive diagnostic feature, the sum of the SB amplitudes, and the measurable nuisance parameter, the power of the mesh harmonic, and continuous adaptation of the technique to changes of the power of the mesh harmonic.
3. A new adaptive diagnostic feature based on the amplitude demodulation of the TSA signals is proposed and investigated. The new diagnostic feature is defined as the ratio of the sum of the sidebands in the envelope spectrum of a mesh harmonic to the measured power of the mesh harmonic.
4. The adaptive demodulation technique is applied to the detection of pitting fault on a back-to-back industrial spur gearbox system and showed effective early differential detection of local tooth pitting. The effectiveness of this detection is evaluated by the Fisher criterion.
5. The adaptive demodulation technique is compared with the classical demodulation technique for experimental pitting detection in conditions of variable mesh amplitudes. It is shown experimentally that the adaptive demodulation technique preserves effectiveness of local fault detection of gears operating in conditions of variable mesh amplitudes.
6. Obviously, the effectiveness of the proposed adaptation depends on error in estimation of the power of mesh harmonic. Therefore, future efforts are needed to investigate this issue.
7. The obtained results confirm previously written findings [8] for non-TSA gear signals. Thus we recommend that one consider using the adaptive demodulation technique as an alternative to the classical demodulation technique.

Acknowledgements

The authors acknowledge the nancial support of the DTI (UK). We also gratefully thank industrial partners for their in-kind support: WYKO (Mr. Brook, Mr. Ohren, Mr. Patel), Severn Trent Water (Mr. Stanley), and Compact Orbital Gears (Mr. LaPayne, Mr. Huges).

6. References

1. R. B. Randall, A new method of modelling gear faults, *Journal of Mechanical Design* 104 (1982) 259-267.
2. P.J. Sweeney, R.B. Randall, Sources of gear signal modulation, *IMechE Second Int. Conf. on Gearbox Noise, Vibration and Diagnostics* (1995) C492/027.
3. P.D. McFadden, Detecting fatigue cracks in gears by amplitude and phase demodulation of the meshing vibration, *Journal of Vibration, Acoustics, Stress, and Reliability in Design* 108 (1986) 165-170.
4. P.D. McFadden, Determining the location of a fatigue crack in a gear from the phase of the change in the meshing vibration, *Mechanical Systems and Signal Processing* (1988) 2(4), 403-409.
5. J.E. Nicks, G. Krishnappa, Gear fault detection using modulation analysis techniques, *IMechE Second Int. Conf. on Gearbox Noise, Vibration and Diagnostics* (1995) C492/033.
6. G. Dalpiaz, A. Rivola, R. Rubini, Effectiveness and sensitivity of vibration processing techniques for local fault detection in gears, *Mechanical Systems and Signal Processing* (2000) 14(3) 387-412.
7. D. Brie, M. Tomczak, H. Oehlmann, A. Richard, Gear crack detection by adaptive amplitude and phase modulation, *Mechanical Systems and Signal Processing* (1997) 11(1) 149-167.
8. L. Gelman, R. Zimroz, J. Birkel, H. Leigh-Firbank, D. Simms, B. Waterland, G. Whitehurst, Adaptive vibration condition monitoring technology for local tooth damage in gearboxes, *Insight International J. of Non-Destructive Testing and Condition Monitoring* 47(8) (2005) 461-464.
9. G. Krishnappa, Gear fault detection parameters development based on modulation techniques. *Fifth International Congress on Sound and Vibration* (1997) 919-926. South Australia, 1997.

10. W. Q. Wang, F. I., M. F. Golnaraghi, Assessment of gear damage monitoring techniques using vibration measurements, *Mechanical Systems and Signal Processing* (2001) 15(5) 905-922.
11. J. Ma, C. J. Li, Gear defect detection through model-based wideband demodulation of vibrations, *Mechanical Systems and Signal Processing* (1996) 10(5) 653-665.
12. P. D. McFadden, Examination of a technique for the early detection of failure in gears by signal processing of the time domain average of the meshing vibration, *Mechanical Systems and Signal Processing* (1987) 1 (2) 173-183.
13. S. Choi, C. J. Li, Estimation of gear tooth transverse crack size from vibration by fusing selected gear condition indices, *Measurement Science and Technology* 17 (2006) 2395–2400.
14. J. Ma, Energy operator and other demodulation approaches to gear defect detection, *Proc. 49th Meeting of the Society of Mechanical Failures Prevention Technology* (1995) 127–140.
15. S. Braun, The extraction of periodic waveforms by time domain averaging. *Acustica* 32 (1975) 69-77.
16. P.D. McFadden, J.D. Smith, Effect of transmission path on measured gear vibration, *Journal of Vibration, Acoustics, Stress, and Reliability in Design* 108 (1986) 377-378.
17. V. A. Kovalevsky, Image pattern recognition. Springer-Verlag, 1980.
18. M. DeGroot, Optimal statistical decisions. McGraw-Hill, 1970.
19. A. Webb, Statistical Pattern Recognition, Arnold, London, 1999.